tour length 10 μm, the estimated molecular weight is 20×10^6. A denatured single strand of contour length 0.5 μm then has a molecular weight equal to 0.5×10^6. These two results imply that the native molecule is assembled from roughly 40 subunits. The absolute molecular weight of native xanthan has not yet been definitely measured. However, Dintzis and his co-workers (*15*) have measured molecular weights of 1.8 to 3.6×10^6 for xanthan solutions prepared by heating xanthan to 90°C for 3 hours in 4*M* urea. Dispersions of xanthan, in 4*M* urea but not heated, gave molecular weights from light scattering of 11 and 50×10^6 for two different samples (*15*). These experiments provide lower and upper limits to the average molecular weight.

One may ask why the particle lengths in the electron micrographs (Fig. 1) differ by a factor of 10 from the hydrodynamic diameter measured by membrane partition chromatography (Fig. 3). It seems most likely that the xanthan structure is not a rigid rod in solution. Rather, it may behave as a wormlike chain similar to DNA, with a small but finite flexibility which allows substantial coiling up at high molecular weight. Under our method of sample preparation for electron microscopy, these coiled molecules become extended. The intrinsic viscosity of xanthan, 4000 to 7000 ml/g (*9*, *16*), is consistent with this wormlike chain model for molecules with a contour length of 2 to 10 μm.

In summary, our observations demonstrate that native exopolysaccharide from *X. campestris* is composed of many subunit strands 2 nm in diameter arranged in a right-handed double or triple helix or, alternatively, a coiled coil having a diameter of 4 nm. Additional experiments will be required to establish the nature of the interchain association and the place of the 3-sugar side chains in the native and denatured molecules.

G. HOLZWARTH
E. B. PRESTRIDGE
Exxon Research and Engineering Company, Post Office Box 45, Linden, New Jersey 07036

References and Notes

1. A. Jeanes, *J. Polym. Sci. Polym. Symp. No. 45* (1974), p. 209.
2. E. I. Sandvik and J. Maerker, in *Extracellular Microbial Polysaccharides*, P. A. Sandford and A. Laskin, Eds. (American Chemical Society, Washington, D.C., 1977), p. 242; G. J. Hirasaki and G. A. Pope, *Soc. Pet. Eng. J.* **14**, 337 (1974).
3. P. E. Jansson, L. Kenne, B. Lindberg, *Carbohydr. Res.* **45**, 275 (1975); L. D. Melton, L. Mindt, D. A. Rees, G. R. Sanderson, *ibid.* **46**, 245 (1976).
4. R. Moorhouse, M. D. Walkinshaw, S. Arnott, *Abstr. Pap. 171st Meet. ACS* (1976), abstract CELL 097.
5. _____, in *Extracellular Microbial Polysaccharides*, P. A. Sandford and A. Laskin, Eds. (American Chemical Society, Washington, D.C., 1977), p. 90.
6. A. Jeanes, J. E. Pittsley, F. R. Senti, *J. Appl. Polym. Sci.* **5**, 519 (1961).
7. D. A. Rees, *Biochem. J.* **126**, 257 (1972).
8. G. Holzwarth, *Am. Chem. Soc. Div. Pet. Chem. Prepr.* **20** (No. 2), 281 (1976).
9. _____, *Biochemistry* **15**, 4333 (1976).
10. E. R. Morris, in *Extracellular Microbial Polysaccharides*, P. A. Sandford and A. Laskin, Eds. (American Chemical Society, Washington, D.C., 1977), p. 81.
11. Xanthan polysaccharide was obtained from Kelco as a dried powder (keltrol) and as a culture broth. The powder was purified by ultracentrifugation, ethanol precipitation, and dialysis, as previously described (*6*, *9*), to remove cells and other fermentation residues. Culture broth was purified by centrifugation to remove cells and by dialysis to eliminate small molecules and ions; this procedure dispenses with all precipitation and drying steps.
12. W. Traub and K. A. Piez, *Adv. Protein Chem.* **25**, 243 (1971); P. D. Ross and J. M. Sturtevant, *Proc. Natl. Acad. Sci. U.S.A.* **46**, 1360 (1960); F. W. Studier, *J. Mol. Biol.* **41**, 199 (1969).
13. M. Dubois, K. A. Gilles, J. K. Hamilton, P. A. Rebers, F. Smith, *Anal. Chem.* **28**, 350 (1956).
14. X-ray work on xanthan fibers (*4*, *5*) is consistent with a fivefold helix of pitch 4.70 nm, which gives a 0.94-nm rise per disaccharide in the main chain. This is quite similar to the rise in cellulose, 1.03 nm. The average molecular weight of a cellobiose unit with its side chain is 936 for the sodium salt of xanthan. This means that the molecular weight per nanometer of contour length must be about 996 for single-stranded fibers, 1992 for double-stranded fibers, and so on.
15. F. R. Dintzis, G. E. Babcock, R. Tobin, *Carbohydr. Res.* **13**, 257 (1970).
16. P. J. Whitcomb, E. J. Ek, C. W. Macosko, in *Extracellular Microbial Polysaccharides*, P. A. Sandford and A. Laskin, Eds. (American Chemical Society, Washington, D.C., 1977), p. 160.
17. We thank J. Ogletree, P. Skiva, and L. Soni for skillful technical assistance and A. I. Laskin for stimulating discussions.

3 March 1977

Bacteria–Plant Cell Surface Interactions: Active Immobilization of Saprophytic Bacteria in Plant Leaves

Abstract. *Fibrillar structures, originating from the plant cell wall in the intercellular spaces of leaves of 'Red Kidney' bean,* Phaseolus vulgaris *L., engulfed a saprophytic bacterium,* Pseudomonas putida, *after its initial attachment to the host walls. Phytopathogenic bacteria,* Pseudomonas phaseolicola *and* Pseudomonas tomato, *did not adhere to the plant cell wall nor were they encapsulated. Bean lectins may be involved in the attachment and encapsulation processes.*

A principle in plant pathology states that pathogenicity is the exception rather than the rule (*1*); plants have defense mechanisms against most microorganisms, and the exception is that pathogens have found ways to circumvent these defenses. One possible defense mechanism would be for a plant to react to "foreign organisms" and immobilize or destroy them. Evidence for such a process was obtained from experiments involving the intromission and subsequent recovery of bacteria from the intercellular spaces of cowpea leaves (*2*). The recovery of pathogenic bacteria was consistently higher than that of saprophytic bacteria. The reduced recovery of saprophytic bacteria occurred within 20 minutes after infiltration, indicating that the saprophytes but not the pathogens were immobilized by a rapid process within the leaves.

We present here evidence that immobilization and encapsulation of a saprophytic bacterium occurs in the intercellular spaces of bean leaves (*Phaseolus vulgaris* L., variety 'Red Kidney'), in contrast to the lack of attachment and encapsulation with pathogens. A related phenomenon has been described in tobacco (*3*, *4*), but the process in beans differs in several important respects from that in tobacco. Preliminary evidence that plant lectins may be involved in the immobilization and encapsulation processes is also presented.

Attached primary leaves of 8-day-old beans grown in a greenhouse were infiltrated with 10^9 bacteria per milliliter by submerging the leaves in the bacterial suspension and applying a vacuum (740 mm-Hg negative pressure) for 2 minutes. *Pseudomonas putida*, a saprophytic bacterium; *Pseudomonas phaseolicola*, a pathogen causing halo blight of beans; and *Pseudomonas tomato*, a pathogen of tomatoes but not of beans, were used in these studies. As the vacuum was released, the suspension moved through the stomata into the intercellular spaces of the leaves. The water-soaked appearance of the leaves disappeared within about 1 hour after incubation in a growth chamber at 24°C, 85 percent relative humidity, and a light cycle of 12 hours per day provided by both fluorescent and incandescent lighting (2.1×10^4 lux). After specified incubation periods from 1 to 30 hours, the leaves were cut into small pieces and fixed with 3 percent glutaraldehyde in 0.1*M* sodium cacodylate buffer (*p*H 7.2) for 4 to 6 hours. The samples were postfixed with 1 percent osmium tetroxide in the same buffer for 2 hours, dehydrated in an ethanol series, and embedded in Spurr's medium (*5*). Thin sections were cut with a diamond knife, stained with uranyl acetate and lead citrate, and observed with an RCA electron microscope.

Attachment of *P. putida* to plant cell walls was observed 1 hour after infil-

tration (Fig. 1A). The initial attachment covered only a small area of the bacterial cell surface, but after 3 hours of incubation, fibrillar bundles that seemed to arise from the cell wall began to cover bacterial cells (Fig. 1 B). The bacterium in Fig. 1C was completely encapsulated after 6 hours of incubation. Figure 1D shows the typical appearance of the encapsulation of a bacterium between the cell walls at the corner of the intercellular spaces 12 hours after infiltration.

Most of the saprophytic bacteria were attached to the walls and became encapsulated. There was no evidence of multiplication in the immobilized bacteria; however, a few of the cells which were not attached to the plant cell walls were occasionally observed dividing 6 hours after infiltration. The leaves inoculated with *P. putida* did not show any symptoms of disease even after several days of inoculation.

Pathogenic bacteria failed to adhere to host cell walls and began dividing after 6 hours. Although numerous bacterial cells were in contact with the plant walls, no encapsulation response occurred. Both bacterial species almost completely filled the intercellular spaces by 24 hours (Fig. 1, E and F), and by this time the internal structure of the plant cells had begun to deteriorate. However, the deterioration processes were different for the two pathogens. Complete disorganization of the cytoplasm occurred with *P. phaseolicola*, and 48 hours after inoculation confluent water-soaked lesions covered most of the leaf surface. With *P. tomato*, the plant cells become highly vacuolated and a cytoplasmic condensation occurred. Shortly after this a hypersensitive response occurred, apparently caused by the high concentration of bacteria used for inoculation.

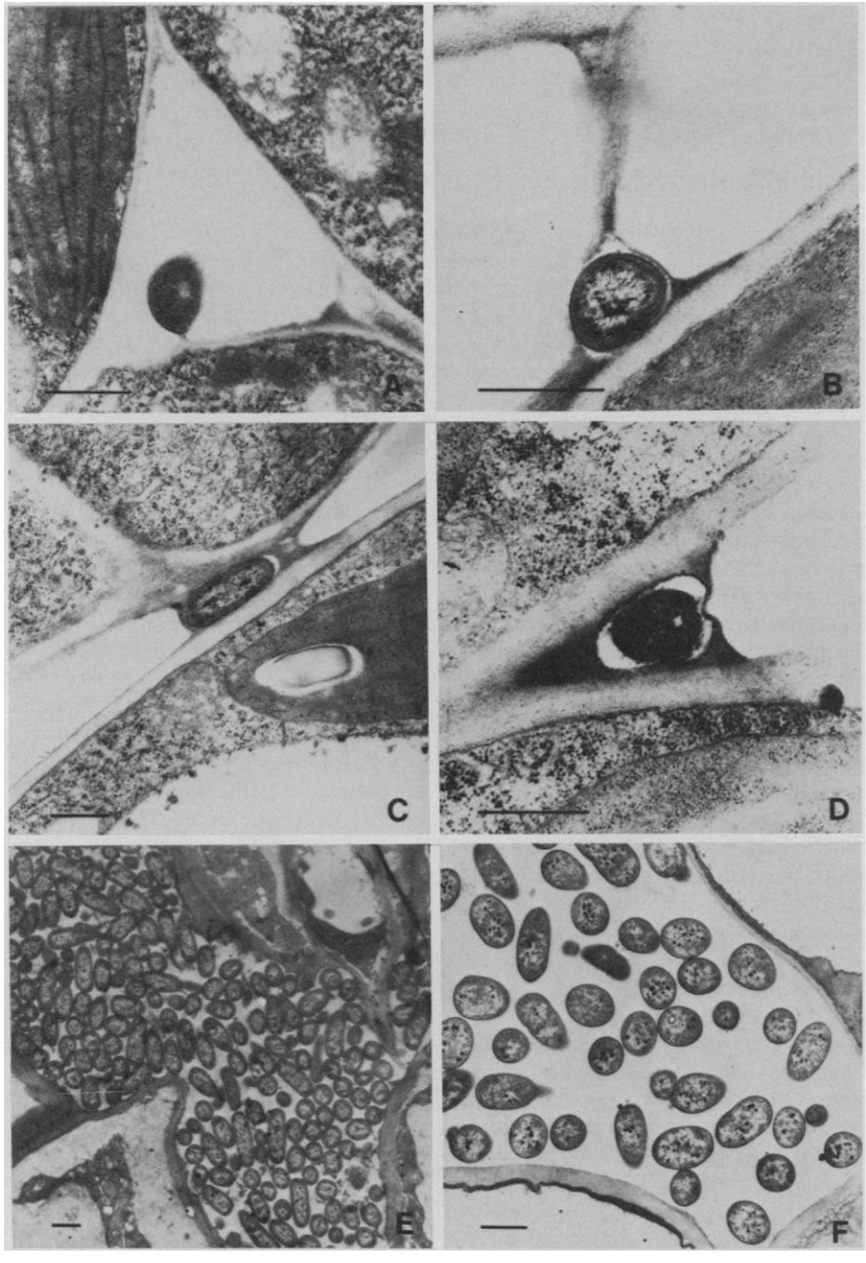

Fig. 1. (A) *Pseudomonas putida* attached to cell wall in the intercellular space 1 hour after infiltration of the bacteria inside the leaf. Note the small area of attachment. (B) Fibrillar bundles arising from the host wall engulf the saprophytic *P. putida* 3 hours after infiltration. (C) Total encapsulation of *P. putida* 6 hours after infiltration. (D) *Pseudomonas putida* 12 hours after infiltration. (E) *Pseudomonas phaseolicola*, a compatible pathogen in beans, almost completely fills the intercellular spaces 24 hours after inoculation. (F) The incompatible pathogen, *P. tomato*, 24 hours after inoculation. Scale bars: (A to D) 0.5 μm, (E and F) 1 μm.

It appears that attachment and encapsulation may be a major defense mechanism in plants against bacteria. The failure of *P. tomato*, a pathogen of tomato but not of bean, to be attached and encapsulated in bean, however, indicates that other defense mechanisms are also operating in this plant. Both preformed and phytoalexin-type compounds have been implicated in plants as chemical defense mechanisms against bacteria (*6*) and one of these mechanisms may prevent *P. tomato* infection of beans.

There is an obvious analogy between the encapsulation of saprophytes by plant leaves and the immune system in animals. The fact that saprophytes are immobilized, whereas pathogens are not, indicates that an active recognition process is involved.

The biochemical basis of the recognition process is open to conjecture. Preliminary experiments suggest that common antigens and lectins may be involved, as they seem to be for the initial recognition between bacterial and plant cell surfaces in other instances (*7*). Bean leaves were infiltrated with a lipopolysaccharide extracted from *P. putida* with phenol. The three bacteria used in our study were infiltrated separately into the leaves 1 hour later. Examination after 6 hours indicated that both the saprophyte and the pathogens were immobilized and encapsulated. Furthermore, fractions P and M of commercially prepared *P. vulgaris* lectins (Bacto-Phytohemagglutinin; Difco) formed precipitation lines with the lipopolysaccharide from both *P. putida* and the pathogens in agar double-diffusion tests. However, only *P. putida* was agglutinated by these lectin fractions. This selective agglutination is similar to the concurrent findings (*8*) that

avirulent strains of *Pseudomonas solanacearum* were agglutinated by potato lectin whereas no agglutination occurred with the virulent strains, even though both strains had a lipopolysaccharide capable of reacting with the potato lectin. However, the virulent strain carried an extracellular polysaccharide that apparently prevented the binding of the lectin to bacterial surfaces (*8*). If the extracellular polysaccharide was removed from the virulent bacteria, they also agglutinated with the potato lectin (*8*). The agglutination of *P. phaseolicola* and *P. tomato* by bean lectins may be prevented by a similar mechanism. If lectins are involved in the initial attachment of bacteria to plant cell walls, the lectins should be present at the surface of the cell wall. To our knowledge, such localization has not been demonstrated.

The encapsulation material has been described in tobacco as a cuticular layer (*3*) or a pellicle surrounding granular material (*4*). In beans there is less evidence of a discrete pellicle and the encapsulation material appears fibrillar rather than granular. Another striking difference between the tobacco and bean systems is in the area of the processes leading to the hypersensitive response. Attachment and encapsulation of avirulent strains of *P. solanacearum* by tobacco cells appear to be essential steps leading to the hypersensitive response (*4*). Attachment and encapsulation of *Pseudomonas pisi* (pathogenic on pea but not tobacco) also takes place in tobacco before the observation of hypersensitivity (*3*). However, *P. tomato* induces the hypersensitive response in the nonhost bean without either attachment or encapsulation of the bacterial cells, and consequently these steps do not appear to be prerequisite for hypersensitivity in 'Red Kidney' beans.

The active and rapid response of the plant cells to saprophytic bacteria make this an interesting system for studying the molecular mechanisms of recognition at the cell surface.

VENANCIO O. SING
MILTON N. SCHROTH
Department of Plant Pathology, University of California, Berkeley 94720

References and Notes

1. C. E. Yarwood, *Phytopathology* **63**, 1324 (1973).
2. D. C. Hildebrand and M. N. Schroth, *ibid.* **58**, 354 (1968).
3. R. N. Goodman, P-Y. Huang, J. A. White, *ibid.* **66**, 754 (1976).
4. L. Sequeira, G. Gaard, G. A. De Zoetten, *Physiol. Plant Pathol.* **10**, 43 (1977).
5. A. R. Spurr, *J. Ultrastruct. Res.* **26**, 31 (1969).
6. D. C. Hildebrand, *Phytopathology* **63**, 301 (1973); N. T. Keen and B. W. Kennedy, *Physiol. Plant Pathol.* **4**, 173 (1974); S. S. Patil and S. S. Gnanamanickam, *Nature (London)* **259**, 486 (1976).
7. J. E. DeVay and H. E. Adler, *Annu. Rev. Microbiol.* **30**, 147 (1976); J. Hamblin and S. P. Kent, *Nature (London)* **245**, 28 (1973); B. B. Bohlool and E. L. Schmidt, *Science* **185**, 269 (1974); *J. Bacteriol.* **125**, 1188 (1976); F. B. Dazzo and D. H. Hubbell, *Appl. Microbiol.* **30**, 1017 (1975); F. B. Dazzo, C. A. Napoli, D. H. Hubbell, *Appl. Environ. Microbiol.* **32**, 166 (1976).
8. L. Sequeira and T. L. Graham, in preparation.
9. The authors are greatly indebted to D. C. Hildebrand for many useful discussions and valuable help in the preparation of this manuscript and to C. E. Ballou, O. C. Huisman, and A. R. Weinhold for their review and critique of the manuscript.

10 March 1977; revised 3 May 1977

Phase Control of Neural Pacemakers

Abstract. *An electrical stimulus resets the phase of a spontaneously rhythmic neuron. The "new phase" versus "old phase" curve shows either of two distinct topological characters, depending on the stimulus magnitude. These features, and a phase singularity implicit in them, are common to many stable oscillations deriving from continuous feedback between two or more biophysical quantities.*

A quarter-century ago, Hodgkin and Huxley (*1*) simultaneously established a paradigm for inquiry into the ionic basis of electrical activity in nerve membrane and gave a quantitative description of action potentials in squid axon, using a system of ordinary differential equations. Their dynamical model (the set of equations) has undergone diverse revisions to improve its precision (for example, by adding a fifth, slower-moving quantity), and to adapt it to use with other cell types and spontaneously rhythmic neurons in which electrical activity pursues a limit-cycle oscillation (*2*).

Except in the boldest simplifications [for example (*3*, *4*)] this class of equations has resisted analytic solution. So with few exceptions its robust or qualitative implications—those that survive the inevitable quantitative adjustments demanded by experimental work—are known only insofar as they are revealed by computer simulation (*5*, *6*), graphical analysis (*7*), and analog devices (*8*).

I report here a robust implication of limit-cycle kinetics in oscillator preparations, such as sensory neurons, spontaneously rhythmic smooth muscle, and the pacemaker regions of the heart. The behavior to be described follows analytically [using the methods of differential topology (*5*, *9*)] from (i) the existence of a limit cycle in the descriptive equations, regardless of the numerical values of measured parameters and of the number of variables encompassed, and (ii) the application of a stimulus which, if sufficiently prolonged, arrests the prior oscillation, regardless of the physical nature of the stimulus. Prolonged hyperpolarization might be an example of such a stimulus. Both (i) and (ii) suffice to account for a newly observed pattern in the way a neural oscillator adjusts the phase of its rhythm after a stimulus impinges on it.

Consider any nerve preparation generating rhythmic action potentials or the smooth subthreshold oscillations revealed by tetrodotoxin in pacemaker membranes (*2*). It will be convenient to take that regular period as our unit of time. Define the instantaneous "phase" as the time elapsed since the most recent voltage maximum (or, in the presence of noise, some best estimate of that time) based on extrapolation of the preceding rhythm. Now let a stimulus impinge on the preparation—for example, an inhibitory postsynaptic potential (IPSP) or a current pulse—following which the preparation soon resumes its previous rhythmic activity, with the same period, but generally with a new phase relative to the extrapolated prior rhythm.

The phenomenon is most readily described in terms of a "resetting curve": a plot of a new phase against an old phase, using data obtained by stimulating at many times in many pacemaker cycles separated by many intervals, as in (*10*, *11*). Just as we extrapolated the prestimulus rhythm forward to estimate the old phase at the stimulus, we now extrapolate the poststimulus rhythm backward to estimate the new phase at the stimulus. In practice (*10–15*), the new phase can be estimated from the timing of only the first poststimulus voltage maximum, if subsequent maxima occur at sufficiently regular intervals [figure 3b in (*12*)]. The shape of this plot depends, of course, on the choice of preparation and the choice of stimulus (such as, a voltage pulse or a burst of inhibitory or excitatory postsynaptic potentials of some duration from some afferent synapse). If, as in the data replotted below from (*10*, *13–16*) and in (*11*, *17*), this curve can be smoothly plotted, then the following features are obtained.

1) The new phase must rise vertically and fall back, or rise or fall through a full cycle, per horizontal cycle of the old phase. This is because the new phase obtained at a given old phase must be the